Materials Today Communications 27 (2021) 102307

Contents lists available at ScienceDirect

Materials Today Communications

journal homepage: www.elsevier.com/locate/mtcomm

Implementation of Abaqus user subroutines and plugin for thermal analysis of powder-bed electron-beam-melting additive manufacturing process

Ning An [a], Guangyu Yang [b], Kun Yang [b], Jian Wang [b], Meie Li [c,*], Jinxiong Zhou [a]

[a] State Key Laboratory for Strength and Vibration of Mechanical Structures and School of Aerospace, Xi'an Jiaotong University, Xi'an 710049, People's Republic of China
[b] State Key Laboratory of Porous Metal Materials, Northwest Institute for Nonferrous Metal Research, Xi'an 710016, People's Republic of China
[c] State Key Laboratory for Mechanical Behavior of Materials, School of Materials Science and Engineering, Xi'an Jiaotong University, Xi'an 710049, People's Republic of China

ARTICLE INFO

Keywords:
Electron beam melting
Additive manufacturing
Finite element method
Thermal analysis
Abaqus

ABSTRACT

Electron beam melting (EBM) is a metal powder bed fusion additive manufacturing (AM) technology that is widely used for making three-dimensional (3D) objects by adding materials layer by layer. EBM is a very complex thermal process which involves several physical phenomena such as moving heat source, material state change, and material deposition. Conventionally, these phenomena are implemented using in-house codes or embedding some user subroutines in commonly used commercial software packages, like Abaqus, which generally requires considerable expertise. Fortunately, recent versions of Abaqus offer a new plugin tool, *AM Modeler*, which provides a rather new and user-friendly method for performing additive manufacturing process simulation. In this work, taking Ti-6Al-4V as the particular example, we present all the details of the finite element (FE) implementation of both Abaqus user subroutines and *AM Modeler* plugin for thermal analysis of EBM additive manufacturing process. The melting pool shape and temperature profiles were predicted and verified against existing literature data. A 3D FE model was also developed to capture the heat transfer features in a real manufacturing process for printing a particular 3D object, "AM" characters, validating the capability of the proposed methods. To facilitate future design and thermal analysis of EBM process and to promote the use of *AM Modeler* plugin, the source codes including Abaqus user subroutines DFLUX and UMATHT as well as Python scripts for implementing *AM Modeler* are made available and could be downloaded from https://github.com/Dr-Ning-An/ebm-abaqus.

1. Introduction

Additive manufacturing, also known as 3D printing, is the construction of complex functional 3D objects from a computer aid design (CAD) model by adding materials layer by layer. EBM is one of the most promising additive manufacturing technologies in which electron beam is used to selectively scan and melt metal powder in a vacuum environment. Since was first introduced in 1997 by Swedish company Arcam AB, EBM has been developed and provides an ideal method for manufacturing light weights, durable and dense end parts which finds many applications in the fields of aerospace and medical implants [1–3]. From initial CAD design to 3D printed part, EBM additive manufacturing process follows a series of steps as described below [4,5]. The building process begins with the deposition of powder layer where solid particles are delivered from the powder hoppers and raked to yield an even layer on the top of the substrate. Next, in preheating, the powder layer is loosely sintered to enable tight stacking through a series of high-energy focused electron beam raster-scanning passages at a high speed. The process is then followed by selective melting and solidification of powder particles by the aid of 3D CAD data. After the completion of one layer building, another layer of powder will again be deposited, preheated, and selectively melted, with the cycle being repeated until the final shape of the desired part is achieved.

From a physical point of view the EBM is a rather complex process involving several thermal phenomena. Heat transfer plays an important role during the whole process, especially for determining the temperature distribution within the model for subsequently predicting evolution of residual stress and deformation [6]. When the electron beam scans on

* Corresponding author.
E-mail address: limeie@mail.xjtu.edu.cn (M. Li).

https://doi.org/10.1016/j.mtcomm.2021.102307
Received 30 December 2020; Received in revised form 31 March 2021; Accepted 31 March 2021
Available online 6 April 2021

the top of the powder layer, the powder particles at the focal spot are heated extremely fast to above their melting temperature, giving rise to the so called *melting pool*. The melting pool moves as the electron beam scans following a prescribed path, part of the heat is lost by radiation from the heated powder to the cooler environment while a large amount of heat is conducted to the surrounding particles and the substrate. There is only a negligible heat loss into the environment by convection, as the process is performed under vacuum [3,7,8]. As the temperature of the melt pool decreases, the fused material then solidifies into a 3D dense part. The melt pool evolution and the material state change from powder to liquid and from liquid to solid comprise the most complex physical aspects in EBM process, and the variation of thermal properties as a function of temperature with respect to material state also complicates the heat transfer problem. Even more effects such as vaporization and scanning strategy should be accounted for in a real additive manufacturing process [9,10].

Finite element method (FEM) is a reliable and efficient way to solve heat transfer problems. Over the past decades, FEM based techniques have been developed by many authors to simulate the EBM process by considering the powder as a continuum when complex geometries are involved and mesoscopic scale model is too expensive (see the review paper of [11,12]). In general, additional special-purpose in-house user subroutines are needed to add capabilities to commonly used commercial software packages for simulating the EBM process. For example, in Abaqus, DFLUX user subroutine is developed to model moving heat source by defining the heat flux distribution as a function of position and time, and UMATHT user subroutine is used to model the material state change and variation of thermal properties as a function of temperature and material state, and a built-in key word *Model Change can be utilized to simulate the layer-by-layer building up process. The development and use of these subroutines generally require considerable expertise in both the theory of thermodynamics and programming in Fortran. Recently, these codes have been incorporated as "internal" user subroutines into an Abaqus plugin – *AM Modeler* – with a graphical user interface (GUI) [13], which would definitely reduce the difficulty of using Abaqus for EBM Modeling. However, compared with the numerous reports on the use of user subroutines [11], very rare studies have described the use of *AM Modeler* [14–16] in EBM process simulation. It could therefore be necessary to document the indications for the use of *AM Modeler* with numerical examples.

In this study, taking Ti-6Al-4V as the particular example, we present in detail the finite element (FE) implementation of both Abaqus user subroutines and plugin tool *AM Modeler* for the thermal analysis of EBM additive manufacturing process. The method of embedding user subroutines into Abaqus to simulate the EBM process has already been proposed and validated by many research teams in recent years [11,12]. It will be convenient, nevertheless, to restate the implementation of Abaqus user subroutines briefly as the simulation results obtained by which are used as reference to verify the effectiveness of *AM Modeler* in present work. We first develop user subroutines, i.e., DFLUX and UMATHT, to investigate the melt pool evolution and temperature profiles of the EBM process and compare our results with existing data obtained from literature for verification. We then apply the *AM Modeler* technique to simulate the same EBM process as previously modeled using user subroutines. Our results indicate that the results obtained using *AM Modeler* are in excellent agreement with that predicted by user subroutines, verifying the use of *AM Modeler*. Finally, by taking advantage of the efficiency of *AM Modeler*, we develop a full 3D FE model to numerically present the complete building process of a particular 3D object, demonstrating the capability of Abaqus AM simulation techniques. We would like to note that all the source codes developed in this work including Abaqus user subroutines DFLUX and UMATHT as well as Python scripts for implementing *AM Modeler* are made available to the research community, with which future researchers do not need to reinvent the wheel. In addition, we hope our efforts would facilitate interaction between academia and industry and boost AM modeling for industrial application purposes.

2. EBM thermal modeling

As discussed in the above section, there are several physical phenomena to be considered in the EBM process including moving heat source, material state change, material deposition, and thermal conduction and radiation, etc. In order to accurately describe the EBM process in an efficient way, we adopt a simplified heat conduction model [5] with appropriate and specific boundary conditions and flux loads (radiation, preheating, electron beam, etc.) as shown in Fig. 1. As a single scan path is simulated in this model, the base material (dark blue) is modeled as a solid substrate, the top thin layer (light blue) is considered as a continuum having the properties of powder, and the electron beam (red spot) occurs at the top surface of the powder layer and travels along the x-axis with a constant speed. We note that the material state change as well as temperature-dependent thermal properties of powder and solid are also accounted for in the model.

(1) Heat transfer equations: In the EBM process, the instantaneous temperature distribution satisfies the following 3D heat transport conduction equation:

$$\rho c_p \frac{\partial T}{\partial t} = k\nabla^2 T + q \tag{1}$$

where ρ is density, c_p is specific heat capacity, T is temperature, k is thermal conductivity, and q is the absorbed heat flux.

The latent heat of fusion, L_f, is considered in this model to trace the solid-liquid interface of the melt pool. When temperature drops to between the solidus and liquidus temperature, T_S and T_L, respectively, the latent heat of fusion is modeled as an additional term of the internal thermal energy per unit mass, dU. Hence, the enthalpy is defined as:

$$H(T) = \int \mathrm{cdT} + L_f f \tag{2}$$

where f is the volumetric fraction of the liquid, which is defined as

$$f = \begin{cases} 0 & T < T_S \\ \dfrac{T - T_S}{T_L - T_S} & T_S \leqslant T \leqslant T_L \\ 1 & T > T_L \end{cases} \tag{3}$$

The radiation between the top surface of the powder layer and surrounding environment is expressed by:

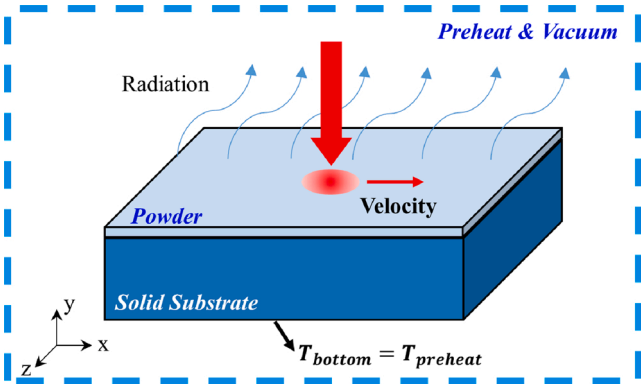

Fig. 1. Illustration of thermal modeling configuration with boundary conditions. The whole model is preheated in a vacuum environment. The top light blue part indicates powder layer, the below dark blue part indicates solid substrate and the red spot indicates the current location of the electron beam. (For interpretation of the references to color in this figure legend, the reader is referred to the web version of this article).

$$-k\frac{\partial T}{\partial n} = \varepsilon\sigma(T^4 - T_e^4) \tag{4}$$

where ε is emissivity, σ is Stefan Boltzmann constant, and T_e is the environmental temperature. In addition, at the bottom surface of the solid domain, a thermal Dirichlet boundary condition with a constant temperature $T_{preheat}$ is applied.

(2) Heat source equations: Two kinds of heat sources are considered in this work: (a) Gaussian heat source model and (b) Goldak heat source model.

(a) Gaussian heat source model is modeled as a conical moving heat source with a Gaussian distribution and parabolically decaying along the beam penetration direction [5]:

$$q(x,y,z) = \eta \times \frac{H_S \times I_Z}{S} \tag{5}$$

with $I_Z = \frac{1}{0.75}\left(-2.25\left(\frac{z}{S}\right)^2 + 1.5\left(\frac{z}{S}\right) + 0.75\right)$ and $H_S = \frac{2UI_b}{\pi\Phi_E^2}\exp\left(-\frac{2[(x-x_0)^2+(y-y_0)^2]}{\Phi_E^2}\right)$ where the parameters include Gaussian distribution function H_S, the parabolic decaying function I_z, electron beam absorption efficiency η, voltage U, current I_b, penetration depth S, beam diameter Φ_E, and the instantaneous horizontal position of the heat source center x_0 and y_0.

(b) Goldak heat source model is also known as double ellipsoidal heat source model [17], in which the distribution of heat fluxes is determined by four geometric parameters including width a, depth b, rear length c_r, and front length c_f, as expressed in Eqs. (6) and (7). Note that $f_r = 2c_r/(c_r + c_f)$ and $f_f = 2c_f/(c_r + c_f)$ are the heat deposited fractional factors in the rear and front quadrant respectively and its sum is equal to 2.

$$q = \begin{cases} q_f, & \text{when} \quad x \geqslant 0 \\ q_r, & \text{when} \quad x < 0 \end{cases} \tag{6}$$

$$q_{f/r} = \frac{6\sqrt{3}f_{f/r}Q}{abc\pi\sqrt{\pi}} e^{\left(-\frac{3x^2}{c_{f/r}^2}\right)} e^{\left(-\frac{3y^2}{a^2}\right)} e^{\left(-\frac{3z^2}{b^2}\right)} \tag{7}$$

(3) Material Properties: The material used in this work is Ti-6Al-4V alloy. Due to the rapid change in temperature during the EBM process, the properties of material should be considered as a function of temperature. Furthermore, the thermal properties of powder are significantly different from those of corresponding solid, and therefore material state change from powder to liquid and then from liquid to solid would also cause changes in material properties. Temperature dependent material properties of both solid and powder (with a porosity of 50%) Ti-6Al-4V used in this work were taken from [5] and summarized in Fig. 2. The specific heat and latent heat of fusion for solid and powder material are considered to be same as many authors did [18,19]. The solidus and liquidus temperature are 1605 °C and 1655 °C, respectively, and the latent heat of fusion is 440 kJ/kg.

To conclude, a successful thermal model for simulating the EBM process must consider three main aspects: (1) an electron beam model representing scanning heat flux input and its movement along the surface; (2) a thermo-physical material model able to represent the different phases of material (powder, solid, liquid) and the material state change (from powder to liquid and from liquid to solid) during the process; and (3) an evolving domain describing the layer build-up process.

3. Finite element simulation techniques

Having introduced thermal modeling of the EBM process, in this section, we move on to present the details on the finite element

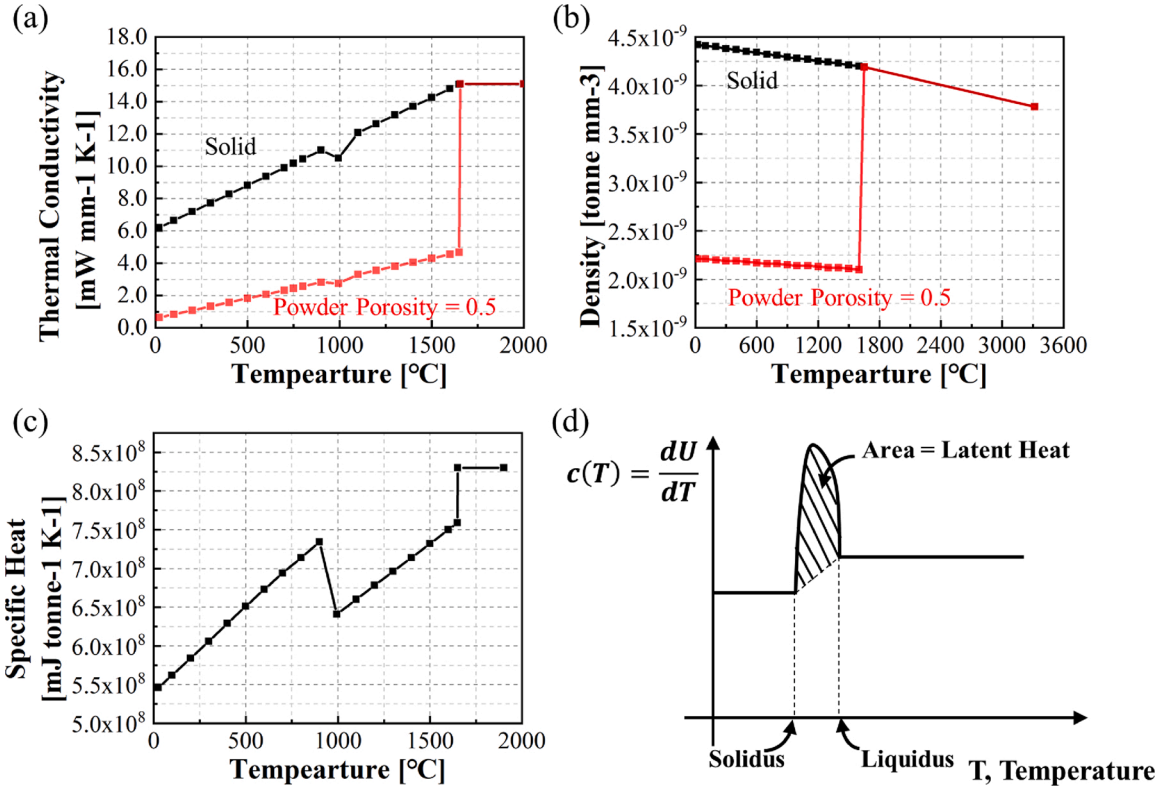

Fig. 2. Temperature dependent material properties of solid and powder (with a porosity of 50%) Ti-6Al-4V. (a) Thermal conductivity, (b) density, (c) specific heat and (d) latent heat.

simulation techniques used to simulate the physical phenomena rising in the EBM process. The core techniques of the implementation of traditional Abaqus user subroutines, i.e., DFLUX and UMATHT, as well as Abaqus new plugin *AM Modeler* for thermal analysis of the EBM process are both summarized as follows.

3.1. User subroutines

(1) DFLUX subroutine: Abaqus DFLUX user subroutines, accounting for both Gaussian and Goldak heat source models, have been developed to model the moving heat sources. To be specific, the DFLUX subroutine is used to define the nonuniform distributed heat fluxes as a function of position and time according to Eqs. (5)–(7). It would be called at the beginning of each time increment and at each flux integration point, and current position of the center of electron beam is determined by the beam scan velocity and simulation time.

(2) UMATHT subroutine: The user subroutine UMATHT has been developed to define the thermal behavior of Ti-6Al-4V (as shown in Fig. 2) as a function of temperature and the material state (powder or solid). A solution-dependent state variable (SDV), named MAT_ID, is created to specify the material state as powder or solid at a time instant. The material state change criterion used by many research teams are slightly different [4,18–22], and in our simulations the criterion proposed by Chou et al. [5,20] was adopted. Initially, the MAT_ID is set to 0 and the powder properties are assigned to the material calculation points of all powder elements. When the powder is melted and under cooling (i.e., $T > T_m$ & $dT/dt < 0$), the MAT_ID changes to 1 and the solid properties are assigned instead. The UMATHT subroutine reads the temperature at each material calculation point at the end of each increment and then updates the MAT_ID value of those material calculation points which meet the state change criterion. Note that the material state change in EBM process can only be one-way (i.e., from powder to solid), which means that the MAT_ID will be locked as 1 whenever it becomes solid. In addition, the UMATHT subroutine also modifies the enthalpy function in order to take into account latent heat effects and the solid fraction during the melting and cooling phases. More details can be found in [5].

3.2. AM Modeler plugin

As implemented in Abaqus 2018 or higher version [23], *AM Modeler* plugin provides new features for the simulation of general additive manufacturing (AM) processes. A number of special-purpose techniques are provided for simulating the EBM process that do not require user to write user subroutines. These new techniques are implemented as "internal" user subroutines in Abaqus using the same user subroutine infrastructure and keyword interface but can be easily accessed by using table collections with reserved string names starting with either "ABQ_AM" or "ABQ_EIG". In order to reflect the physical aspects as mentioned in previous section, two basic ingredients are offered by the new techniques, which are progressive element activation for simulating controlled deposition of raw materials, and moving heat fluxes for modeling electron beam-induced heating in a thermal analysis.

Taking advantage of *AM Modeler*, three new data types have been introduced to manage input data for the EBM process simulation. *(i) Event Series.* The event series can be imaged as a combination of path and amplitude. Time (t) and position (x, y, z) are mandatory columns in an event series for defining the time and space variation of event path, and user defined dependent variables can also be added to prescribe the corresponding amplitude. In our simulations, two event series with input files are defined for respectively simulating the deposition of raw powder layers and the movement of electron beam. Specifically, roller event series is used to define the motion of powder recoater and Goldak event series is used to define the moving path and powder amplitude of

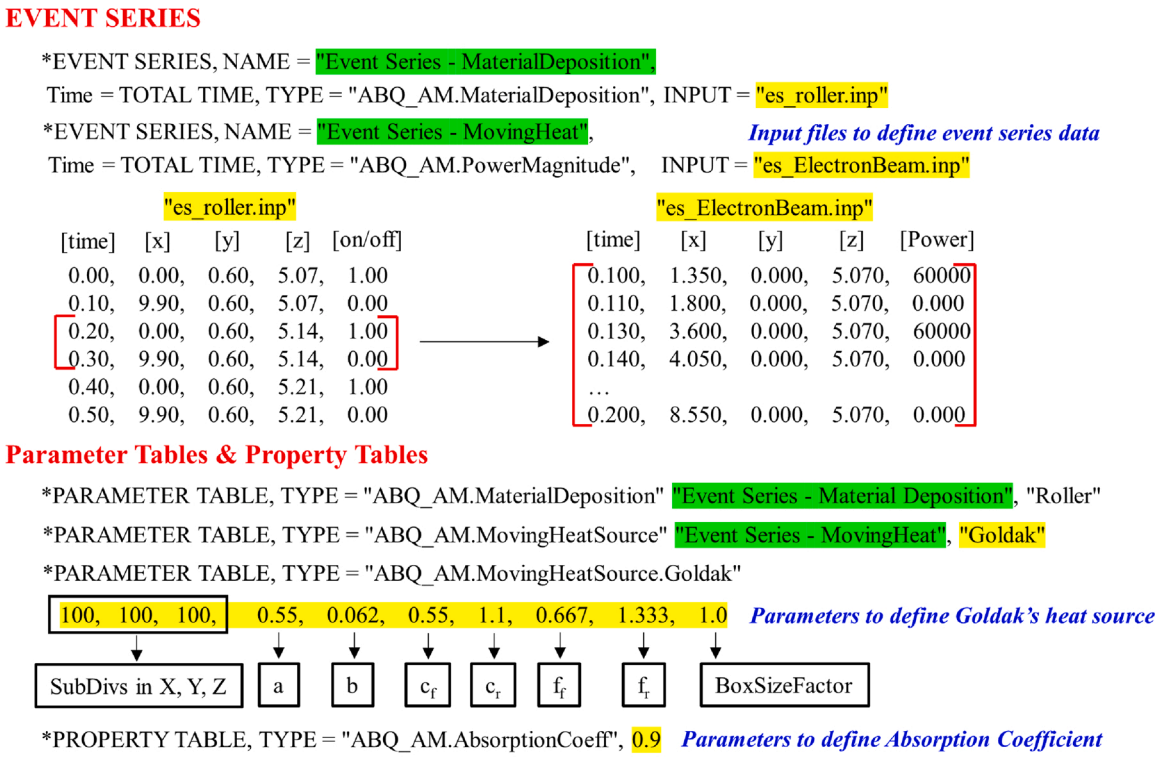

Fig. 3. Data structures to manage input data in *AM Modeler* for the EBM process simulation.

the electron beam. Examples of input files for each event series are shown in the top panel of Fig. 3. *(ii) Parameter table.* The parameter table collects all the necessary parameters for performing an event. For example, in the middle panel of Fig. 3 we present the parameter table used for defining a Goldak heat source model which includes all the parameters as depicted by Eq. (7). *(iii) Property table.* The property table is used to define dependent parameters which could be dependent on temperature, field and SDVs. For example, the heat absorption coefficient in moving heat source modeling is defined using property table. All the parameter tables and property tables are eventually encapsulated in a table collection for each event as shown in the bottom of Fig. 3.

4. Verification and validation of FE simulation techniques

4.1. FE simulation model

In order to verify the accuracy of the proposed FE simulation techniques, the EBM process of Ti-6Al-4V alloy was investigated by using both Abaqus user subroutines and *AM Modeler* plugin. The FE model was realized by 3D solid elements with type DC3D8 for uncoupled heat transfer analysis in Abaqus 2020. Fig. 4 shows the FE model with mesh transition and boundary conditions. The FE model consists of a solid substrate with dimensions of 21 mm × 2.5 mm × 10 mm ($x \times y \times z$) and a powder layer with dimensions of 21 mm × 2.5 mm × 0.07 mm. The electron beam heating occurs at the left top corner of the powder layer [position (0, 0, 10.07)] and travels along the x-axis with a constant speed. Because of a high energy intensity and a fast travel speed in EBM, temperature gradients are expected to be very high, and thus finer meshing is required along the electron beam scanning path; coarser meshing is then used in the regions away from the heat affected zone. Specifically, the element size in the scanning area is 50 μm × 50 μm × 17.5 μm with mesh size gradually increases with the distance away from the primary scanning area and the total element number is 132, 435. A symmetric boundary condition was applied to the surface of $y = 0$ mm, and a thermal Dirichlet boundary condition with a constant temperature of 730 °C was applied to the surface of $z = 0.0$ mm, and radiation boundary conditions were applied to the top surface of powder layer with an emissivity of 0.7.

4.2. Verification of FE simulation techniques

We began by considering a simple case by assuming the materials are all solid, i.e., solid properties were assigned to both the substrate and the top layer. In this case, the material heated by the electron beam experiences a phase change from solid to liquid and from liquid to solid ("S-L-S"). This is not realistic; however, it is very appropriate for use in the verification of user subroutines DFLUX and UMATHT by performing two specific simulation jobs. In the first job, material properties were input directly through Abaqus GUI, while in the second job they were input through UMATHT subroutine. In accordance with [5], a Gaussian distributed heat source with parameters listed in Table 1 was implemented using DFLUX subroutine for both jobs. The melting pool shape and temperature profile were predicted. The results obtained from two jobs match excellently with each other and are both in very good agreement with the numerical results reported by Cheng et al. [5] as shown in Fig. 5a and c. We also find that by using UMATHT it takes approximately 2.7 times CPU time as long as by using Abaqus GUI to input the material properties, but the use of UMATHT makes it possible to define a material state change in further analysis from powder to liquid and from liquid to solid ("P-L-S") in order to represent the physics of EBM process, which cannot be achieved by merely using Abaqus GUI. We then consider the "P-L-S" case in which solid properties were assigned to the solid substrate via Abaqus GUI and powder properties were assigned to the powder layer via UMATHT and a solution-dependent variable (MAT_ID) was used to update the material state. The simulation results are also in good agreement with the numerical and experimental results reported in [5] as shown in Fig. 5b and d.

Table 1
Parameters of Gaussian Heat Source taken from [5].

Parameters	Values
Electron beam diameter, Φ (mm)	0.55
Absorption efficiency, η	0.9
Scan speed, v (mm/s)	632.6
Beam voltage, U (kV)	60
Beam current, I_b (mA)	6.7
Beam penetration depth, S (mm)	0.062

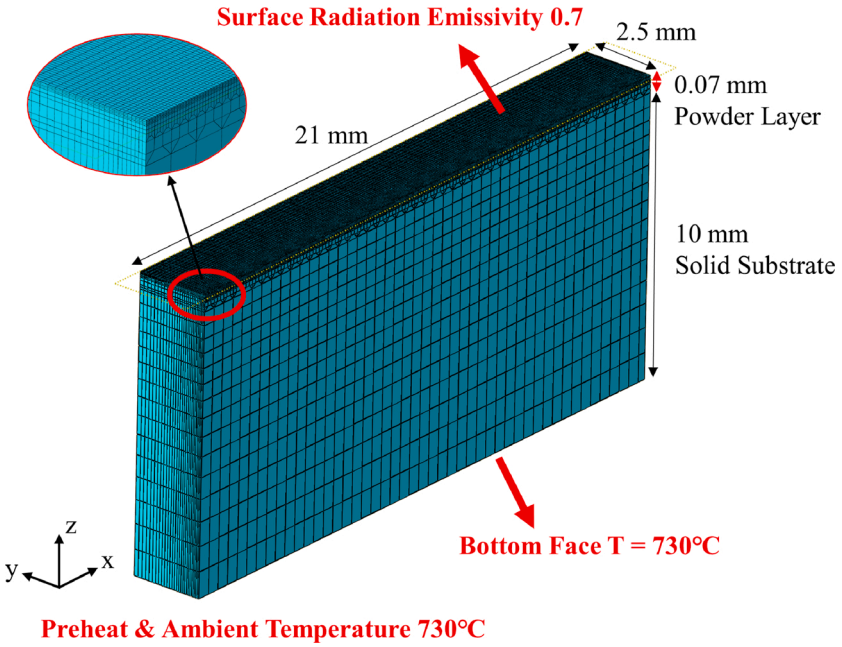

Fig. 4. Three dimensional FE model for thermal analysis of EBM process with boundary conditions.

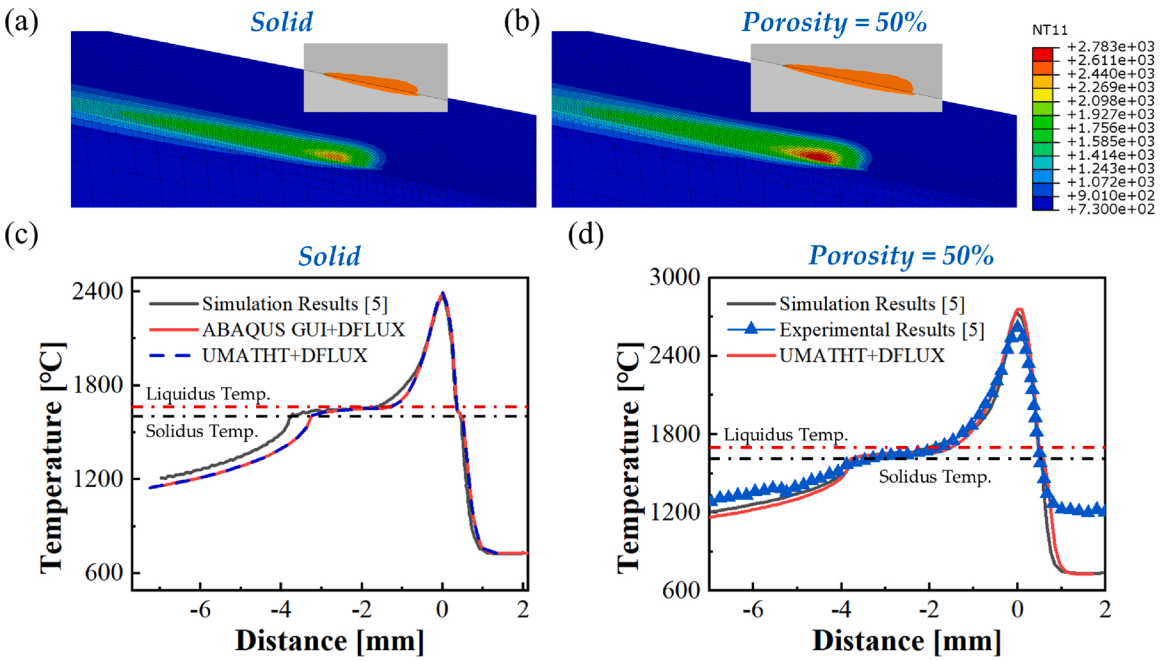

Fig. 5. Temperature contour with melting pool shape and temperature profile along beam center scan pass. (a) and (c) Solid properties were assigned to the top layer and the material heated by electron beam experienced a phase change from solid to liquid, and from liquid to solid ("S-L-S"). The results obtained by using Abaqus GUI and UMATHT are both in good agreement with the numerical results reported in [5]. (b) and (d) Powder properties were assigned to the top layer and the material heated by electron beam experienced a phase change from powder to liquid, and from liquid to solid ("P-L-S"). The results obtained by using combined UMATHT and DFLUX are in good agreement with the numerical and experimental results reported in [5].

Next, to verify the accuracy of *AM Modeler*, we consider another "P-L-S" case where a Goldak's double ellipsoidal heat source model was employed to simulate the heat fluxes within the same FE model. The parameters of Goldak's heat model are presented in Fig. 3. An event series for simulating the movement of electron beam was defined so that the electron beam moves along the *x*-axis with a constant speed of 632.6 mm/s and the power amplitude was set to 200 W. A DFLUX user subroutine was also developed to model the Goldak's heat source for comparison. The simulation results obtained from using *AM Modeler* and DFLUX are in a very good agreement, as shown in Fig. 6.

4.3. Validation of FEM simulations

Having verified the accuracy of the proposed FE simulation techniques, we then applied these techniques to model the EBM additive manufacturing process of two 3D characters "AM", as an example to validate the capability of the proposed methods. In this case, user subroutine UMATHT was adopted to define the material state change of "P-L-S" and *AM Modeler* was employed to define the deposition of powder layers and Goldak's moving heat source. In Fig. 7 we show the investigated geometry with tool path of event series. The powder layers were added sequentially on a solid substrate of 9.9 mm × 1.2 mm × 5.0 mm (length × width × height). The powder part has a height of 4.2 mm which is composed of 60 powder layers and each layer has a height of 0.07 mm. The element size of powder layer along the height direction is set to 0.035 mm; in such a way, two layers of elements represent one physical layer of powder. The powders elements were activated layer by layer according to the movement of the recoater blade defined by a "Roller" event series as the tool path shown in Fig. 7a. The deposition of each powder layer was then followed by selective melting by electron beam following the prescribed path as depicted in Fig. 7b.

Fig. 8 shows the FE snapshots of the EBM additive manufacturing process at various step times. Blue in Fig. 8 represents a MAT_ID value of 0, which the indicates initial deposited powder layers. As the electron beam moves along the prescribed path, the powder material located in the path were heated by the electron beam and experienced a state

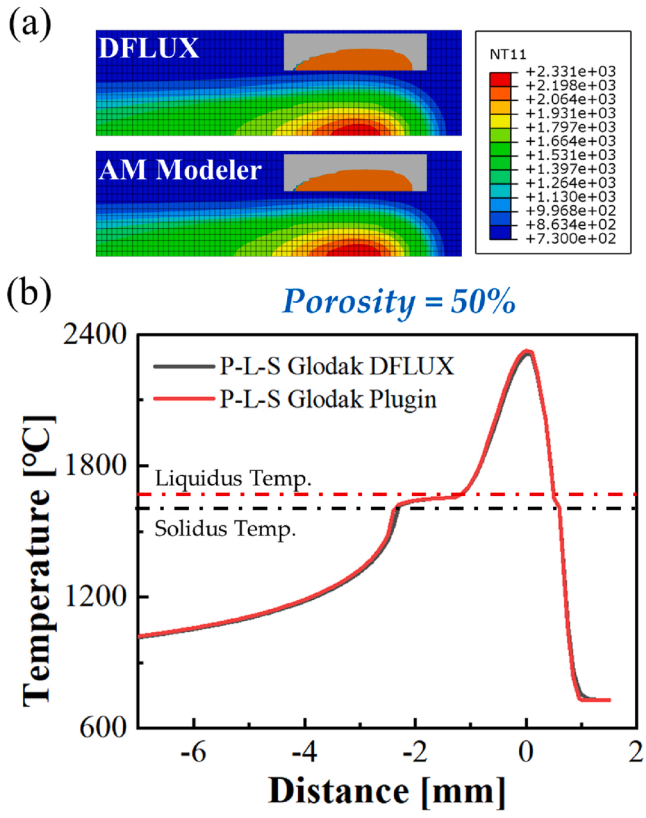

Fig. 6. "P-L-S" simulation results by Goldak's double ellipsoidal heat source model predicted using DFLUX and *AM Modeler*. (a) Temperature contour with melting pool shape indicated by orange in the inserted image and (b) temperature profile along beam center scan pass. (For interpretation of the references to color in this figure legend, the reader is referred to the web version of this article).

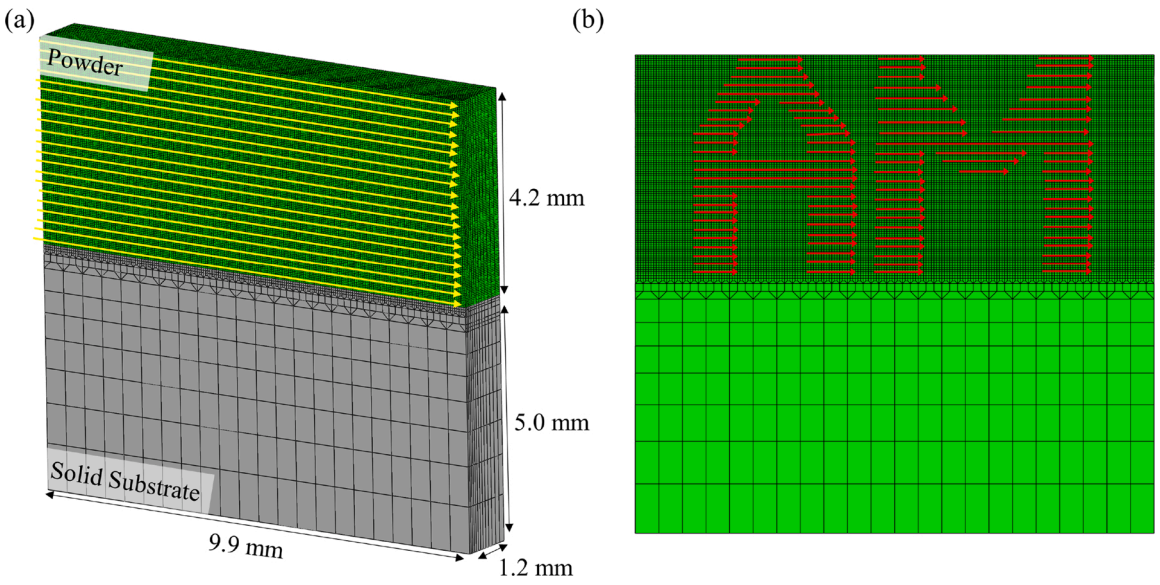

Fig. 7. Tool path of event series for (a) progressive elements activation and (b) moving heat source.

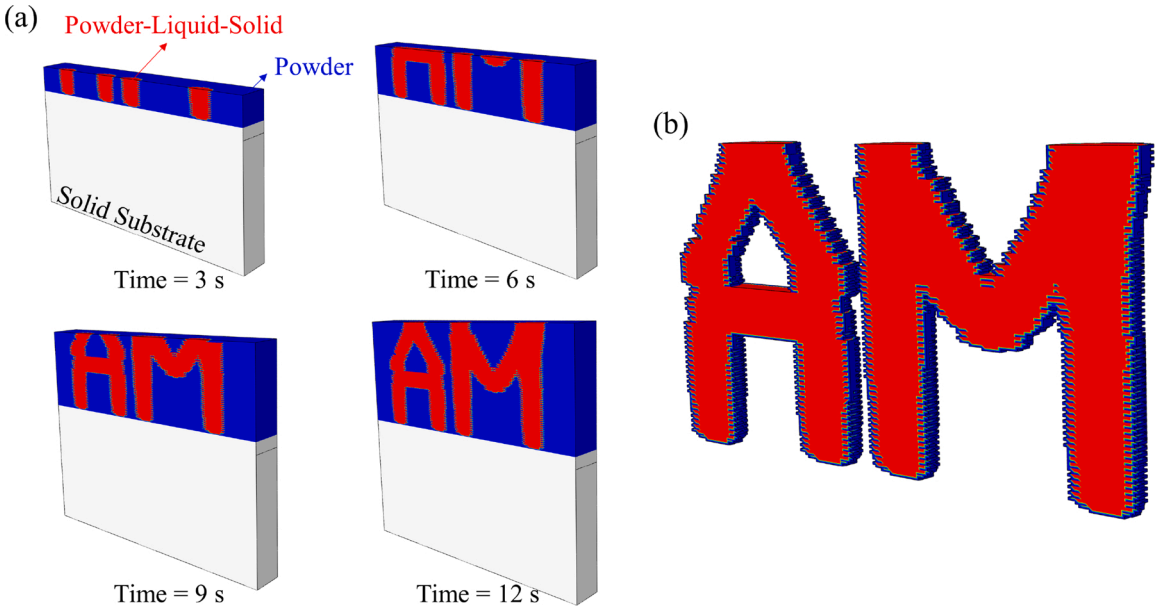

Fig. 8. FE simulation demonstration for 3D printing "AM" characters. (a) FE snapshots of the EBM additive manufacturing process with distribution of MAT_ID value. Red represents a Mat_ID value of 1, indicating solid, and blue represents a Mat_ID value of 0, indicating powder. (b) The final 3D "AM" characters object manufactured from the EBM process. (For interpretation of the references to color in this figure legend, the reader is referred to the web version of this article).

change of "P-L-S". The color of these materials was turned into red, which represents a MAT_ID value of 1 and indicates these materials have been solidified. Fig. 8b presents the final design of the 3D printed "AM" characters object. The outer surfaces of the object are quite rough due to the layer by layer nature of the deposition techniques and post-treatments are usually needed for improving the surface quality of additive manufactured metallic parts [24].

5. Conclusion

Within this study, we present the implementation of Abaqus user subroutines and plugin tool for thermal analysis of EBM additive manufacturing process. There are three main physical aspects during the EBM process, which are moving heat source, material state change, and material deposition. From a computational point of view, a few finite element based simulation techniques are proposed to model these physical aspects and simulate the EBM process. In specific, DFLUX user subroutines are developed for modeling the moving electron beam heat source, UMATHT user subroutines are programmed for modeling the material state change and the use of *AM Modeler* plugin for integrated simulation of moving heat source and depositing powder materials is also detailed. The simulation results with the use of subroutines and *AM Modeler* plugin were verified against existing numerical and experimental data from the literature. The simulation techniques are then applied to simulate the heat transfer phenomena in the EBM additive manufacturing process of 3D printing of "AM" characters.

The simulation results demonstrate the capability of the proposed simulation techniques. We only model Ti-6Al-4V alloy but the proposed method can be extended to other materials readily. We conclude that the simulation techniques developed within this work is a sufficient method

for thermal analysis of the EBM additive manufacturing process. We hope our efforts contribute to the enhancement of understanding of the EBM process and provide helpful case studies and available source codes for users either from academia or industry.

Data availability

The raw/processed data required to reproduce these findings are available to download from [https://github.com/Dr-Ning-An/ebm-abaqus].

Conflict of interest

The authors declare no conflict of interest.

Declaration of Competing Interest

The authors report no declarations of interest.

Acknowledgement

This research is supported by a Science Challenge project (TZ2018006) and by National Natural Science Foundation of China (grant 11972277).

References

[1] Arcam website, http://www.arcam.com (accessed 12.11.20).
[2] V. Bhavar, P. Kattire, V. Patil, S. Khot, K. Gujar, R. Singh, A review on powder bed fusion technology of metal additive manufacturing, 4th International Conference and Exhibition on Additive Manufacturing Technologies-AM-2014 (2014) 1–2.
[3] L.-C. Zhang, Y. Liu, S. Li, Y. Hao, Additive manufacturing of titanium alloys by electron beam melting: a review, Adv. Eng. Mater. 20 (5) (2018) 1700842.
[4] M.F. Zäh, S. Lutzmann, Modelling and simulation of electron beam melting, Prod. Eng. 4 (1) (2010) 15–23.
[5] B. Cheng, S. Price, J. Lydon, K. Cooper, K. Chou, On process temperature in powder-bed electron beam additive manufacturing: model development and validation, J. Manuf. Sci. Eng. 136 (6) (2014).
[6] P. Prabhakar, W.J. Sames, R. Dehoff, S.S. Babu, Computational modeling of residual stress formation during the electron beam melting process for inconel 718, Addit. Manuf. 7 (2015) 83–91.
[7] E. Landau, E. Tiferet, Y. Ganor, R. Ganeriwala, M. Matthews, D. Braun, M. Chonin, G. Ziskind, Thermal characterization of the build chamber in electron beam melting, Addit. Manuf. 36 (2020) 101535.
[8] M. Galati, A. Snis, L. Iuliano, Powder bed properties modelling and 3d thermo-mechanical simulation of the additive manufacturing electron beam melting process, Addit. Manuf. 30 (2019) 100897.
[9] Y. Lee, M.M. Kirka, J. Ferguson, V.C. Paquit, Correlations of cracking with scan strategy and build geometry in electron beam powder bed additive manufacturing, Addit. Manuf. 32 (2020) 101031.
[10] Y. Liu, S. Li, H. Wang, W. Hou, Y. Hao, R. Yang, T. Sercombe, L.C. Zhang, Microstructure, defects and mechanical behavior of beta-type titanium porous structures manufactured by electron beam melting and selective laser melting, Acta Mater. 113 (2016) 56–67.
[11] M. Galati, L. Iuliano, A literature review of powder-based electron beam melting focusing on numerical simulations, Addit. Manuf. 19 (2018) 1–20.
[12] Z. Luo, Y. Zhao, A survey of finite element analysis of temperature and thermal stress fields in powder bed fusion additive manufacturing, Addit. Manuf. 21 (2018) 318–332.
[13] D. Systemes, Abaqus Analysis User's Guide 2020, Simulia Inc., Providence, RI, USA, 2020.
[14] A. Cattenone, S. Morganti, G. Alaimo, F. Auricchio, Finite element analysis of additive manufacturing based on fused deposition modeling: distortions prediction and comparison with experimental data, J. Manuf. Sci. Eng. 141 (1) (2019).
[15] Y. Yang, M. Allen, T. London, V. Oancea, Residual strain predictions for a powder bed fusion inconel 625 single cantilever part, Integr. Mater. Manuf. Innov. 8 (3) (2019) 294–304.
[16] X. Song, S. Feih, W. Zhai, C.-N. Sun, F. Li, R. Maiti, J. Wei, Y. Yang, V. Oancea, L. R. Brandt, et al., Advances in additive manufacturing process simulation: residual stresses and distortion predictions in complex metallic components, Mater. Des. (2020) 108779.
[17] J. Goldak, A. Chakravarti, M. Bibby, A new finite element model for welding heat sources, Metall. Trans. B 15 (2) (1984) 299–305.
[18] C. Fu, Y. Guo, Three-dimensional temperature gradient mechanism in selective laser melting of ti-6al-4v, J. Manuf. Sci. Eng. 136 (6) (2014).
[19] J. Seon Ho, P. Eun Gyo, K. Jae Won, J.Y. Kim, E. Lee, J.Y. Cho, J.H. Kim, et al., Thermal analysis of metal additive manufacturing process with consideration of density change, in: APISAT 2019: Asia Pacific International Symposium on Aerospace Technology, Engineers Australia, 2019, p. 627.
[20] N. Shen, K. Chou, Thermal modeling of electron beam additive manufacturing process: powder sintering effects, in: International Manufacturing Science and Engineering Conference, vol. 54990, American Society of Mechanical Engineers, 2012, pp. 287–295.
[21] M. Galati, L. Iuliano, A. Salmi, E. Atzeni, Modelling energy source and powder properties for the development of a thermal fe model of the ebm additive manufacturing process, Addit. Manuf. 14 (2017) 49–59.
[22] I. Sani, Selective Laser Melting Process Simulation: Advancements Towards a Cost-Effective Model, Ph.D. Thesis, Istituto Universitario di Studi Superiori di Pavia, 2017.
[23] DASSAULT SYSTENES, "Additive Manufacturing," [Online]. Available from: http://www.3ds.com/products-services/simulia/trends/digital-additive-manufacturing/ (accessed 12.11.20).
[24] E. Maleki, S. Bagherifard, M. Bandini, M. Guagliano, Surface post-treatments for metal additive manufacturing: progress, challenges, and opportunities, Addit. Manuf. (2020) 101619.